Role of phorbol ester localization in determining protein kinase C or RasGRP3 translocation: Real-time analysis using fluorescent ligands and proteins

Derek C. Braun,[1,2] Yeyu Cao,[4] Shaomeng Wang,[4] Susan H. Garfield,[3] Gang Min Hur,[2] and Peter M. Blumberg[2]

[1]Department of Biology, Gallaudet University, Washington, District of Columbia; Laboratories of [2]Cellular Carcinogenesis and Tumor Promotion and [3]Experimental Carcinogenesis, National Cancer Institute, NIH, Bethesda, Maryland; [4]Departments of Internal Medicine and Medicinal Chemistry and Comprehensive Cancer Center, University of Michigan, Ann Arbor, Michigan

Abstract

The diacylglycerol signaling pathway, involving protein kinase C (PKC) and RasGRP, is a promising therapeutic target for both cancer and other indications. The phorbol esters, ultrapotent diacylglycerol analogues, bind to and activate PKC and RasGRP. Here, using fluorescent phorbol esters and complementary fluorescent PKC and RasGRP constructs, we determined the localization of the phorbol ester as a function of time after addition and how the resultant PKC or RasGRP3 translocation related to ligand localization. For these studies, we prepared fluorescently labeled phorbol esters of varying lipophilicities based on the BODIPY FL (green) or BODIPY 581/591 (red) fluorophores, and by using fusion constructs of green fluorescent protein or DsRed with PKC isoforms or RasGRP3 expressed in Chinese hamster ovary cells, we simultaneously compared the kinetics and pattern of localization of PKC or RasGRP3 with that of the fluorescent red or green phorbol esters. Binding assays showed that the fluorescent derivatives were potent ligands. Uptake followed a one-compartment pharmacokinetic model with a half-time of minutes to hours, depending on the ligand, and all of the fluorescent phorbol esters localized primarily to intracellular membranes, with little plasma membrane localization. The fluorescent phorbol esters induced translocation of and generally colocalized with PKCδ or RasGRP3. However, PKCα and, initially, PKCδ, translocated to the plasma membrane, in which little phorbol ester accumulated. The findings argue that the rate of uptake of phorbol esters influences the subsequent pattern of PKCδ translocation, and that the specificity for PKCα translocation is dominated by factors other than the localization of the ligand. [Mol Cancer Ther 2005;4(1):141–50]

Introduction

The lipophilic second messenger *sn*-1,2-diacylglycerol (DAG) regulates a broad range of cellular functions, including tumor promotion, apoptosis, differentiation, and growth. The responses to DAG are mediated by a superfamily of receptors that include the protein kinase C (PKC) family of serine/threonine kinases (1, 2) and the RasGRP family of Ras guanyl nucleotide exchange factors (3–6). The DAG-sensitive isozymes of PKC include the calcium-dependent classic PKCs (α, β_I, β_{II}, γ) and the calcium-independent novel PKCs (δ, ε, η, θ; 1). The DAG receptors each contain one or more highly conserved C1 domains, zinc finger motifs that act as the binding site for DAG and the phorbol esters, ultrapotent analogues of DAG (7, 8).

Because of its roles in cell proliferation, differentiation, and apoptosis, PKC has attracted considerable interest as a potential target for cancer chemotherapy. Overexpression of specific PKC isoforms can cause malignant transformation of cells, and altered expression of specific PKC isoforms has been described in multiple tumor types (9). The effects of PKC are isoform, cell type, and context specific. For example, in glioma cells PKCδ is proapoptotic in response to etoposide but antiapoptotic in response to Sindbis virus (10). Similarly, PKCα induces hormone-independent proliferation in breast cancer (11) but inhibits proliferation in malignant melanoma (12). In numerous systems, PKCs also stimulate multidrug resistance (13). The context-dependent role of individual PKC isozymes in different cell types affords wide opportunities for design of drug specificity.

Currently, several chemotherapeutic agents targeting PKC are in various stages of development. There are both examples of agents that activate or inhibit PKC, and some show isoform selectivity. These agents include the PKC activators bryostatin 1, phorbol 12-myristate 13-acetate (PMA), and ingenol 3-angelate (14–16); the antisense oligonucleotides aprinocarsen and Affinitak (LY900003; ISIS 2521; ref. 17, 18); and agents that potentiate cytotoxic drugs, such as UCN01, PKC412, and tamoxifen (9, 19). Data on the Adriamycin derivative AD 198 show specific PKC targeting and suggest an improved therapeutic profile over traditional anthracyclines (20). Finally, drugs targeting PKC are being evaluated for pathologies other than cancer: these

Received 8/4/04; revised 10/15/04; accepted 11/8/04.

The costs of publication of this article were defrayed in part by the payment of page charges. This article must therefore be hereby marked advertisement in accordance with 18 U.S.C. Section 1734 solely to indicate this fact.

Requests for reprints: Peter M. Blumberg, National Cancer Institute, NIH, Building 37, Room 4048, 37 Convent Drive, MSC 4255, Bethesda, MD 20892-4255. Phone: 301-496-3189; Fax: 301-496-8709. E-mail: blumberp@dc37a.nci.nih.gov

include LY333531 for diabetic retinopathy and renopathy (21) and prostratin and 12-deoxyphorbol 13-phenylacetate for HIV in conjunction with highly active antiretroviral therapy (22, 23).

The hallmark of activation by DAG or phorbol ester is the translocation of the receptor to a subcellular compartment or membrane, in which the activated receptor may phosphorylate substrates or interact with target proteins in a location-dependent fashion. Fusion proteins between green fluorescent protein (GFP) and PKC have proven of great value for characterizing this translocation (24). The sites of translocation of receptor as well as the rapidity of translocation following treatment with phorbol ester both differ depending upon the specific phorbol ester (25–27). Using a series of symmetrical phorbol esters that varied in acyl chain length and lipophilicity, our laboratory previously showed that the pattern of PKCδ translocation in response to phorbol ester treatment was dependent on the lipophilicity of the phorbol ester. The lipophilic phorbol esters induced initial translocation of GFP-tagged PKCδ to the plasma membrane, whereas the more hydrophilic phorbol esters resulted in initial translocation to the nuclear membrane (26).

Localization of activated PKCs, as well as their persistence within a location, should determine their access to different substrates and thereby may affect their selectivity of activation of downstream cellular pathways. A better understanding of the factors driving PKC and RasGRP3 translocation may allow us to better understand how different phorbol esters show selectivity in their activation of downstream cellular pathways although they may exhibit similar *in vitro* binding affinities. This knowledge, in turn, should facilitate the design of more selective drug candidates targeted to the DAG signaling pathway (28).

In this study, we did real-time analysis of the pharmacokinetics and intracellular migration of phorbol esters by using a series of brightly fluorescent phorbol ester derivatives. These fluorescent derivatives have allowed us to visualize the entry of phorbol ester into the cell, to determine the distribution of phorbol ester within the cell as a function of time, and to correlate these data with the kinetics and localization of different phorbol ester receptors before and after drug exposure. These studies provide new insight into the pharmacology of the phorbol esters.

Materials and Methods

Materials

PMA and phorbol 12,13-dibutyrate (PDBu) were obtained from LC Laboratories (Woburn, MA). [^{3}H]PDBu was obtained from New England Nuclear (Shelton, CT). Enzymes for molecular cloning and PCR were purchased from New England Biolabs (Beverly, MA), Invitrogen (Carlsbad, CA), and Roche Molecular Biochemicals (St. Louis, MO). Primers were purchased from Invitrogen.

Cell Culture, Bacterial Strains, Transfection, and Transformation

CHO-K1 cells (CCL 61) were obtained from the American Type Culture Collection (ATCC, Manassas, VA). Cells were cultured at 37°C in Kaighn's modification of Ham's F12 medium adjusted to contain 1,500 mg/L of sodium bicarbonate (ATCC), and supplemented with 10% fetal bovine serum (FBS, Invitrogen) in a humidified atmosphere containing 5% CO_2. Cultured cells were grown to 90% confluence before transfection. Transient transfection was done with LipofectAMINE 2000 (Invitrogen) according to the manufacturer's directions. All experiments were done the day after transfection. *Escherichia coli* DH5α-MCR was grown at 37°C in Luria-Bertani medium, either in broth or on agar. Kanamycin was used in Luria-Bertani medium at a concentration of 50 μg/mL and ampicillin at 100 μg/mL. Recombinant DNA transformation of *E. coli* DH5α-MCR was done according to the heat-shock protocol (29).

Construction of Plasmids

GFP fusions of PKCα, PKCδ, and RasGRP3 had been constructed previously in our laboratory (6, 29). We constructed DsRed fusions by amplifying PKCα, PKCδ, and RasGRP3 from their parent plasmids, using primers with compatible flanking restriction sites and then inserting the amplicons into either pDsRed-N1 or pDsRed2-N1 (Clontech, Palo Alto, CA). Successful construction was verified by restriction digestion, sequencing, and functional testing to see if the novel plasmids, expressed in CHO-K1 cells, exhibited translocation of fusion protein after treatment of the cells with 1 μmol/L PMA.

Molecular Biology Methods

Plasmid DNA was purified chromatographically by using commercial kits from Qiagen (Valencia, CA). Polymerase chain reactions were done with *PfuUltra* high-fidelity DNA polymerase (Stratagene, La Jolla, CA) according to the manufacturer's directions.

Binding of [^{3}H]PDBu

[^{3}H]PDBu binding was measured by using the polyethylene glycol precipitation assay developed by our laboratory (30). Dissociation constants (K_i) of ligands were determined by competition of [^{3}H]PDBu binding to receptor. Recombinant PKCα and PKCδ were expressed in Sf9 insect cells and partially purified as described briefly (31), whereas RasGRP3 was expressed in *E. coli* as a maltose-binding protein fusion protein (pMAL system, New England Biolabs) and purified by affinity chromatography according to the manufacturer's instructions. The assay mixture (250 μL) contained 50 mmol/L Tris-Cl (pH 7.4), 100 μg/mL phosphatidylserine, 4 mg/mL bovine IgG, [^{3}H]PDBu, and variable concentrations of competing ligand. Incubation was carried out at 37°C for 5 or 30 minutes. Samples were chilled on wet ice for 5 minutes followed by the addition of 200 μL of 35% polyethylene glycol in 50 mmol/L Tris-Cl (pH 7.4). The samples were incubated on wet ice for another 10 minutes. The tubes were centrifuged at 12,400 × *g* for 15 minutes at 4°C. Aliquots (100 μL) of the supernatant were pipetted into scintillation vials to determine the free concentrations of [^{3}H]PDBu. The tips of the centrifuge tubes, containing the pellets, were excised, carefully dried, and transferred to scintillation vials for quantitation of the total bound [^{3}H]PDBu. CytoScint ES (ICN Biomedicals, Aurora, OH)

was added to all the scintillation vials before counting. Nonspecific binding was determined by using an excess (40 μmol/L) of nonradioactive PDBu. Specific binding was calculated as the difference between total and nonspecific binding.

In a typical competition assay, eight concentrations of the competing ligand were used. ID_{50} values were determined from the competition curve by nonlinear multiple regression analysis. The K_i for the competing ligand was calculated from its ID_{50} by using the relationship

$$K_i = \frac{ID_{50}}{1 + (\frac{L}{K_d})}$$

where L is the concentration of free [^{3}H]PDBu and K_d is the dissociation constant. Values represent the mean of triplicate experiments, as indicated, with triplicate determinations of each point in each competition curve in each experiment.

Determination of log $P_{o/w}$

The octanol/water partition coefficient, log $P_{o/w}$, for BODIPY FL was determined by using the shake-flask method. First, the respective peak absorbance wavelengths and extinction coefficients for BODIPY FL in octanol-saturated water and in water-saturated octanol were determined. Using these parameters, we measured spectrophotometrically the concentration of solute in the octanol and water partitions after 1 hour of shaking. We thus obtained a log $P_{o/w}$ value of -1.11 ± 0.15 ($n = 3$) for BODIPY FL. Incorporating this value, we predicted the log $P_{o/w}$ of the fluorescent phorbol esters, using the LogKow software package (Syracuse Research Corporation, North Syracuse, NY), which is based on the algorithm of Meylan and Howard (32). The predicted lipophilicity for PE-BDFL-C2 was empirically verified by the shake-flask method and found to be very similar to that predicted by our calculations (log $P_{o/w}$ of 2.21 versus 2.25, respectively).

Uptake Assays

CHO-K1 cells were seeded on 96-well plates, grown overnight, and the medium replaced with 200 μL of DMEM supplemented with 20% FBS. Fluorescent phorbol ester was diluted in Dulbecco's PBS, and, immediately upon starting the assay, 50 μL of each dilution was added to each experimental well. Dulbecco's PBS containing an equivalent amount of DMSO was added to each blank well. Each experiment consisted of triplicate experimental wells and triplicate blank wells. Readings were taken on an fmax fluorescence microplate reader (Molecular Devices, Sunnyvale, CA), kept at a constant temperature of 37°C for 21 or 31 intervals over the period of the assay. Under these conditions, phorbol ester uptake is represented as

$$[D] \xrightarrow{k} [C]$$

where C is the intracellular concentration of phorbol ester, the dose D is the concentration in the extracellular environment, and k is the rate of uptake. In our experiments, we assumed that the dose D remains constant due to the large volume of drug-containing medium in proportion to the small volume of cells. We verified this assumption for PE-BDFL-C2; its concentration remained within 0.3% of its original value over an incubation time of 60 minutes ($n = 3$ experiments). Incorporating time, t, and an intracellular/extracellular equilibrium coefficient, E, we modeled the kinetics as

$$\frac{dC}{dt} = k(E \cdot P - C)$$

Solving for C by Laplace transformation yielded

$$C = E \cdot P \cdot (1 - e^{-kt})$$

Data were entered into Microcal Origin 6.0 graphing software (Microcal Software, Northampton, MA), and values of $E{\cdot}D$ and k were determined by curve fitting by the Levenberg-Marquardt least squares algorithm to the equation described above.

Visualization by Confocal Microscopy

Before observation, the cells were washed twice in DMEM without phenol red, supplemented with 1% FBS. The temperature was kept steady at 37°C throughout all experiments. Fluorescent cells were examined with a Zeiss LSM 510 confocal imaging system (Carl Zeiss Inc, Thornwood, NY) with an Axiovert 100M inverted microscope operating with a 25-mW argon laser tuned to 488 nm and a 1-mW HeNe laser tuned to 543 nm. Cells were imaged with a 63 × 1.4 NA Zeiss Plan-Apochromat oil-immersion objective. Images were collected by using a multitrack configuration in which the green and red emission was collected in PMT 3 with a BP 505-550 filter and PMT 1 with a LP560 filter, after excitation with the 488- and 543-nm laser lines, respectively.

Results

Synthesis of Green and Red Fluorescent Phorbol Esters

Fluorescent phorbol esters have proven to be valuable tools in the analysis of PKC (33). In the present study, we synthesized a series of brightly fluorescent phorbol esters of varying lipophilicities that would be suitable for imaging in live cells and compatible with simultaneous imaging with GFP or DsRed fusion proteins. The derivatives incorporated the BODIPY FL and BODIPY 581/591 (34) fluorophores into the phorbol ester together with variable hydrophobic elements. The synthetic approach was to first introduce a short chain into the phorbol ester, which converted the highly masked hydroxyl group of the phorbol ester core to an easily accessed terminal amine, followed by coupling with the fluorophore and removal of the protecting group (Fig. 1). The fluorophore was separated from the phorbol ester core by variable lengths of methylene spacer, which provided different lipophilicities

(Fig. 1). To determine the lipophilicities of our compounds, we first empirically measured the lipophilicity of BODIPY FL then used this value to calculate the lipophilicities of the fluorescent phorbol esters via the LogKow software package (see Materials and Methods). The predicted lipophilicity for PE-BDFL-C2 was verified empirically and found to be very similar to that predicted by our calculations (log $P_{o/w}$ of 2.21 versus 2.25, respectively). The lipophilicities of the compounds synthesized ranged from log $P_{o/w}$ of 2.25 to 8.64.

Binding Properties of Fluorescent Phorbol Esters to PKCα, PKCδ, and RasGRP3

To determine whether the fluorescent phorbol esters retained activity despite the addition of the somewhat bulky BODIPY fluorophore and spacer, the fluorescent phorbol esters were assayed for binding affinities to purified PKCα, PKCδ, and RasGRP3. Because we wished to relate these results to biological responses such as PKC translocation at early times, incubation times were for 5 minutes. The apparent K_i values were in the nanomolar range (1.4 to 210 nmol/L), indicating that these phorbol esters possessed significant potency, although all were less potent than PDBu (Table 1). The relationship between K_i and phorbol ester lipophilicity seen with these fluorescent derivatives showed that the apparent K_i values increased (apparent potency decreased) with phorbol ester lipophilicity for all three receptors that were tested.

Lipophilic phorbol esters dissolve poorly in the aqueous phase (35) and require a longer incubation period to transfer to the membrane to bind receptor (26). Therefore, we also assayed the apparent K_i values for PKCδ after 30 minutes of incubation. Apparent K_i values measured under these conditions showed increased apparent binding potencies for the lipophilic phorbol esters, such that the K_i values became more similar across different

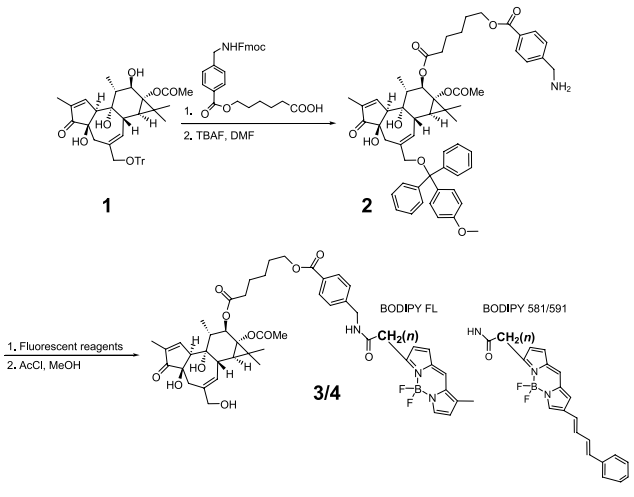

Figure 1. Synthesis of fluorescent phorbol esters. A series of six novel phorbol esters covalently linked to either the green fluorescent BODIPY FL (*top*) or the red fluorescent BODIPY 581/591 fluorophore (*bottom*) were synthesized. The log $P_{o/w}$ values were calculated as described in Materials and Methods.

lipophilicities (see Table 1). These results predict that the more lipophilic derivatives will require more time to partition to the cell membrane and correspondingly will show delayed uptake and cause delayed translocation.

Kinetics of Uptake of Fluorescent Phorbol Esters

The fluorescent phorbol esters gave us the opportunity to determine the kinetics of uptake of the compounds into cells and to determine how uptake depended on lipophilicity and culture conditions. The kinetics of uptake of the red and green phorbol esters over time were quantitated via microtiter fluorimetry and by laser scanning confocal microscopy. In early experiments, it became apparent that the presence of FBS in the culture medium had a marked influence on the uptake kinetics, simplifying the kinetics such that it fit a one-compartment pharmacokinetic model (data not shown). Because phorbol esters may bind to surfaces and, depending on lipophilicity, may dissolve poorly in the aqueous phase, we hypothesized that the bioavailability of the phorbol esters was influenced by serum proteins, with likely candidates being albumin or α_1-acidic glycoprotein (orosomucoid). We measured uptake kinetics in the presence of different concentrations of bovine serum albumin (5–25 mg/mL) or orosomucoid (2–500 μg/mL) alone and found that, of these two, only orosomucoid enhanced uptake and facilitated the shifting of kinetics to a one-compartment curve (data not shown). Because fitting to a one-compartment model enabled the determination of the rate of uptake and the equilibrium coefficient, we did subsequent uptake experiments in medium supplemented with 20% FBS.

Our results show that the equilibrium coefficient, E, and the rate of uptake, k, were constant at different doses within the range of 250 nmol/L to 1 μmol/L. In addition, quantitative experiments using confocal microscopy yielded equivalent measurements of k. We were unable to evaluate the highly lipophilic phorbol esters PE-BDFL-C15 and PE-BD581-C10 because they did not dissolve appreciably in medium and no measurable uptake was seen (Fig. 2; Table 1).

The kinetics of uptake depended on lipophilicity. The more hydrophobic phorbol esters showed slower uptake kinetics, with a 23-fold difference in k between the most hydrophilic (log $P_{o/w}$ = 2.25) and most hydrophobic (log $P_{o/w}$ = 6.18) phorbol ester whose rates of uptake we were able to measure. The half-time ($t_{1/2}$), calculated from k, ranged from 4 minutes for PE-BDFL-C2 to 140 minutes for PE-BDFL-C10. The equilibrium coefficient, E, increased somewhat with the lipophilicity of the phorbol ester (from 11.60 for PE-BDFL-C2 to 21.63 for PE-BDFL-C10, a 2-fold increase) but not to the extent expected from the log $P_{o/w}$ value.

Intracellular Distribution of Fluorescent Phorbol Ester

Using a homologous series of nonfluorescent phorbol esters that varied in lipophilicity, we had determined in a previous study that the membrane localization of PKCδ was dependent on both the ligand and on time. Using fluorescent phorbol esters, we wished to determine

Table 1. The binding properties and uptake kinetics of the fluorescent phorbol esters

Ligand	log $P_{o/w}$	Receptor binding (K_i, nmol/L)				Uptake kinetics		
		RasGRP, 35-min	PKCα, 5-min	PKCδ, 5-min	PKCδ, 30-min	E	k (min^{-1})	$t_{1/2}$ (min)
PDBu (K_d)		0.94 ± 0.02	0.30 ± 0.05	0.39 ± 0.004				
Ligands with a green BODIPY FL fluorophore								
PE-BDFL-C2	2.25	5.7 ± 1.2	1.4 ± 0.1	3.0 ± 0.2	1.5 ± 0.1	11.6 ± 1.3	0.18 ± 0.024	4
PE-BDFL-C4	3.23	12.7 ± 0.7	6.0 ± 0.3	4.8 ± 0.4	2.8 ± 0.2	16.0 ± 0.9	0.13 ± 0.036	6
PE-BDFL-C10	6.18	5.7 ± 0.7	16.0 ± 0.5	8.1 ± 0.4	2.2 ± 0.0	21.6 ± 2.5	0.0049 ± 0.00083	140
PE-BDFL-C15	8.64	92.7 ± 3.9	211 ± 17	199 ± 26	31.2 ± 6.3			
Ligands with a red BODIPY 581/591 fluorophore								
PE-BD581-C4	5.44	21.1 ± 0.5	10.8 ± 2.3	8.6 ± 0.8	1.4 ± 0.4	11.7 ± 0.4	0.0123 ± 0.0006	56
PE-BD581-C10	8.32	210 ± 20	86.6 ± 4.4	71.0 ± 6.9	24.4 ± 2.2			

NOTE: For PDBu, K_d values are shown for comparison. For uptake kinetics, E represents the equilibrium coefficient, k represents the rate of uptake, and $t_{1/2}$ represents the half-life, as determined using 1 μmol/L of fluorescent ligand. Empirically determined values for K_i, E, and k are the mean ± SE for three or more experiments.

whether phorbol esters of differing lipophilicity differentially localized to cellular membranes, because this could explain the differential localization observed for PKCδ. Cells were treated with fluorescent phorbol ester and examined by laser scanning confocal microscopy to determine the intracellular distribution as a function of time. Indeed, all of our fluorescent phorbol esters localized similarly within the cell (Fig. 3), although they differed in their relative rates of uptake (Table 1; Figs. 4 and 5). Overlapping phase contrast and fluorescence confocal images show that the primary destination for the fluorescent phorbol esters was to the perinuclear area, presumably the proximal endoplasmic reticulum, and the nuclear membrane. Phorbol ester did not localize visibly within the nucleus and also did not accumulate visibly in the plasma membrane.

Distribution of Fluorescent Phorbol Ester and GFP- or DsRed-Tagged Receptor Protein as a Function of Time

Using both fluorescent phorbol ester and fluorescent receptor, we were able to simultaneously compare the kinetics of distribution of ligand and receptor. CHO-K1 cells were transfected with plasmids expressing fusions of

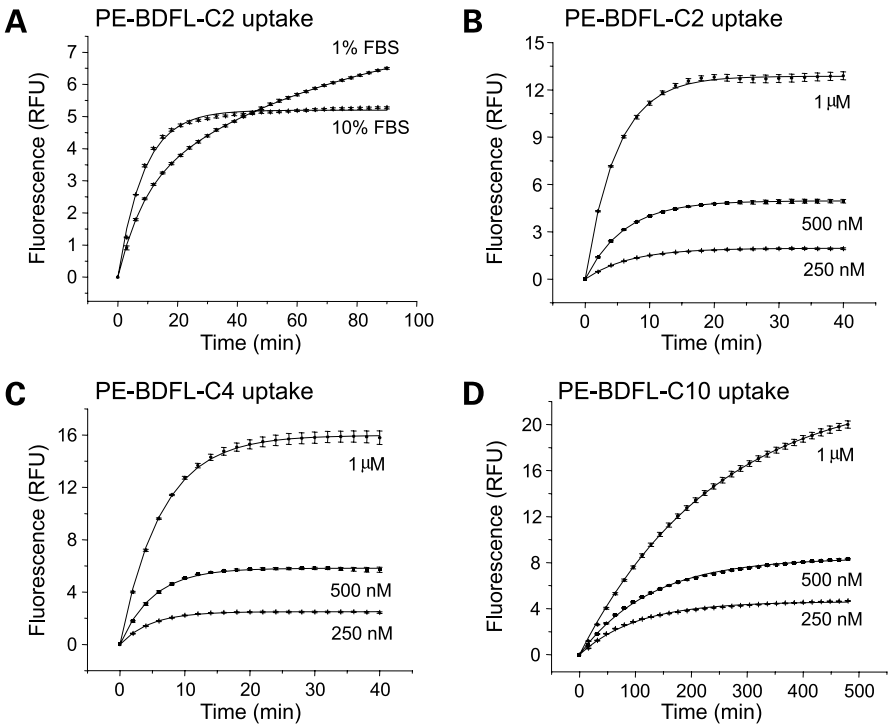

Figure 2. Uptake assays. Uptake assays were done as described in Materials and Methods. Fluorescence is measured in relative fluorescence units (RFU). **A,** uptake of PE-BDFL-C4 in the presence of 1% FBS versus 10% FBS; **B, C,** and **D,** representative uptake assays for three different ligands at 1, 500, and 250 nmol/L of fluorescent phorbol ester. All experiments were repeated two or more additional times with similar results.

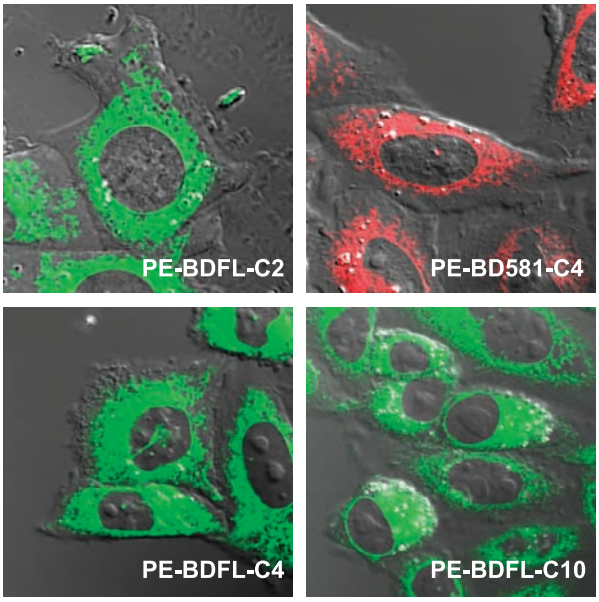

Figure 3. Equilibrium distribution of fluorescent phorbol ester. Cells were incubated in 1 μmol/L fluorescent phorbol ester for time $\geq t_{95\%}$, calculated mathematically from k (see Table 1). Images were recorded by laser scanning microscopy with a phase contrast overlay (see Materials and Methods). Two or more additional experiments with each ligand yielded similar results.

PKCα, PKCδ, or RasGRP3 receptor to either enhanced GFP or DsRed. Cells were treated with fluorescent phorbol ester and visualized in real time by laser scanning confocal microscopy.

RasGRP3 receptor and fluorescent phorbol ester colocalized and comigrated to the perinuclear area (see Fig. 4). In many experiments, an identical clumped distribution of RasGRP3 and phorbol ester was seen, emphasizing a high degree of colocalization. The pattern of intracellular distribution of phorbol ester and RasGRP3 was consistent across phorbol esters of different lipophilicities, but varied in the rate of phorbol ester uptake and the time required for nuclear translocation (~10 minutes for PE-BDFL-C2 compared with ~60 minutes for PE-BDFL-C10).

Fluorescent phorbol ester induced patchy translocation of PKCα to the plasma membrane and colocalized with PKCα at the plasma membrane for a duration that depended on the lipophilicity of the phorbol ester (see Fig. 4). This was followed by accumulation of phorbol ester in the perinuclear area, whereas PKCα and some amount of phorbol ester remained colocalized at the plasma membrane. As predicted from the results with the fluorescent ligands by themselves, the hydrophilic phorbol esters showed more rapid uptake and accumulation in the perinuclear area.

It should be noted that the distribution of fluorescent phorbol ester in the presence of overexpressed PKCα was somewhat different from that observed in the absence of overexpressed PKCα, in which case fluorescent ligand was not seen at the plasma membrane. We assume that this reflects the enhanced presence of ligand at the cytoplasmic membrane due to its binding to overexpressed receptor. Unfortunately, because of the inability to fix the phorbol ester, it is not possible to use immunocytochemistry to simultaneously measure the localization of the fluorescent ligand and of endogenous PKC.

Phorbol ester induced translocation of PKCδ in a lipophilicity-dependent manner and remained colocalized with PKCδ throughout translocation (see Fig. 5). The hydrophilic phorbol esters showed perinuclear colocalization with PKCδ, whereas the hydrophobic phorbol esters showed initial cytoplasmic membrane and some perinuclear colocalization with PKCδ, which over time progressed to primarily perinuclear colocalization. As with PKCα, the initial accumulation of the fluorescent phorbol ester at the plasma membrane together with the PKCδ presumably reflected its trapping by the PKC. The more rapid penetration of the hydrophilic phorbol ester provided an alternative site of translocation of the PKCδ to internal membranes and thereby drove its localization to the internal sites.

Discussion

Our laboratory had previously shown that the pattern and rate of translocation of a PKCδ-GFP fusion protein expressed in cultured cells differed depending on the lipophilicity of the phorbol ester used to treat the cells (26). We hypothesized that lipophilicity of a phorbol ester may influence its rate of penetration, its equilibrium concentration in intracellular spaces, and its pattern of intracellular distribution, and this, in turn, may have determined or influenced the translocation patterns of GFP-PKCδ that were observed in that study. To find the correlation between translocation kinetics and these parameters, we synthesized a series of red and green brightly fluorescent phorbol esters that differed from one another in their respective lipophilicities (log $P_{o/w}$ ranged from 2.25 to 8.64). Although the range of properties of the compounds was limited by the available BODIPY derivatives, we were able to make green derivatives spanning a broad range of lipophilicities and to obtain two red derivatives.

Binding assays showed that these fluorescent phorbol esters acted as potent ligands for the receptors (K_i values ranged from 5.7 to 209 nmol/L). We showed that the more lipophilic derivatives transferred slowly to the lipid phase *in vitro* to bind with an apparent greater potency on incubation for 30 minutes (K_i values ranged from 1.5 to 31.2 nmol/L). This slow transfer to the lipid phase would correspondingly be expected to cause slow uptake and translocation and therefore would be an important contributor to the pattern of biological responses to such ligands. Early studies have identified the problem of low aqueous solubility of typical phorbol esters (35, 36), but the contribution of this low solubility to subsequent responses has not received much attention.

Our uptake experiments done in real time, by microplate fluorimetry and confocal microscopy, showed that

the fluorescent phorbol esters entered cells slowly, and indeed that the highly lipophilic phorbol esters entered very slowly, with a $t_{1/2}$ of 140 minutes reported for our most lipophilic derivative that we could measure. In addition, the lipophilic phorbol esters equilibrated at higher levels within the intracellular membranes (measured values for E ranged from 11.60 to 21.63), although the difference was not as great as would be expected based on their octanol/water partition coefficients (log $P_{o/w}$ for the compounds that we were able to test ranged from 2.25 to 6.18). These findings are important because many responses to the phorbol esters that are of interest are both rapid and then desensitize (e.g., induction of *fos*). Our findings predict that hydrophilic and hydrophobic derivatives will differentially modulate acute versus more long-term responses. This prediction remains to be tested directly, however.

Our direct measurements of uptake with the use of fluorescent phorbol esters verify indirect indications with nonfluorescent phorbol esters suggesting slow penetration. Murphy et al. had shown that the more lipophilic phorbol esters induced responses in rat brain cortex synaptosomes

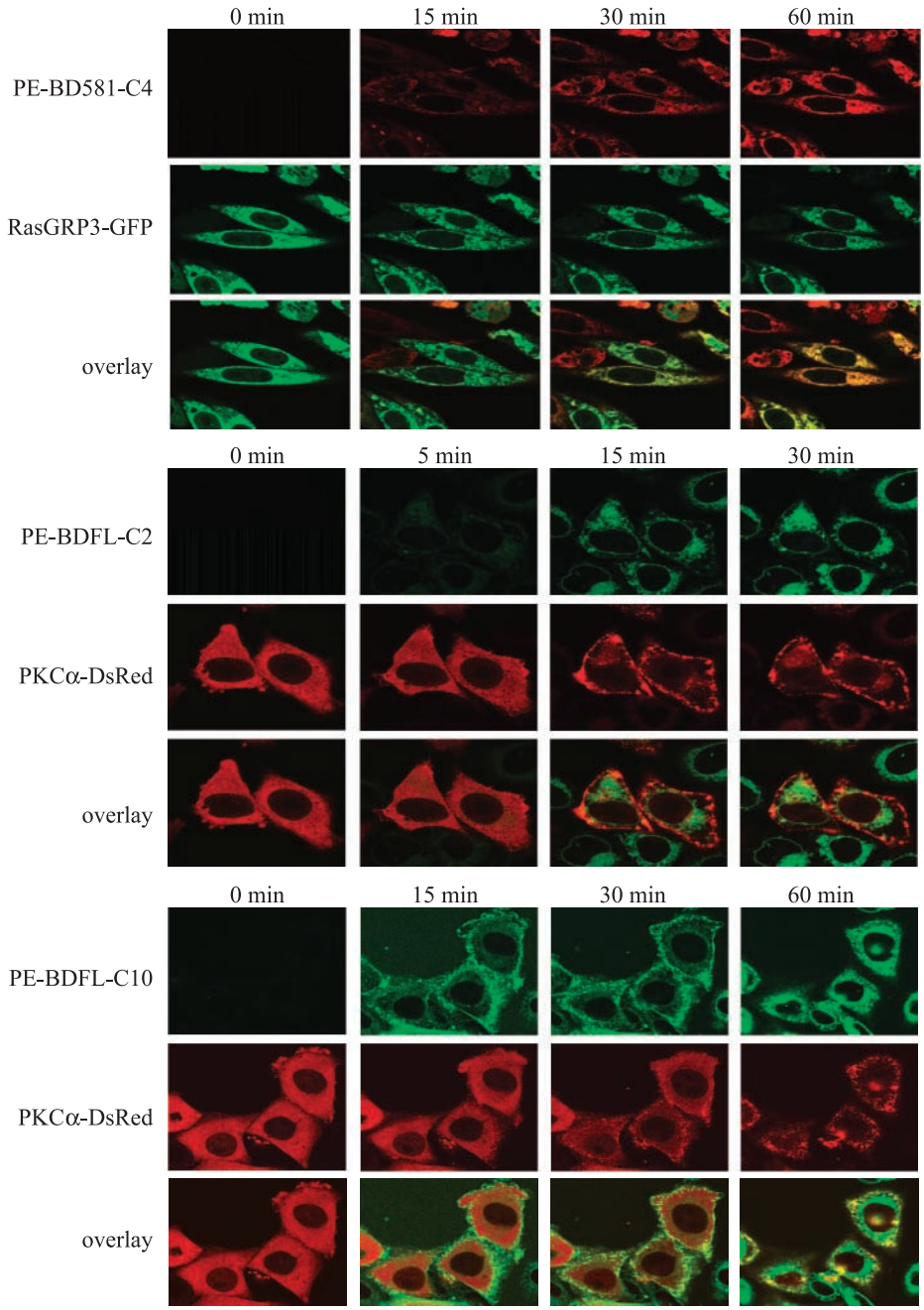

Figure 4. Real-time visualization of fluorescent phorbol ester with green-tagged RasGRP3 or red-tagged PKCα. CHO cells expressing GFP-RasGRP3 or DsRed-tagged PKCα were incubated in 1 μmol/L fluorescent phorbol ester. Images were recorded by laser scanning microscopy as described in Materials and Methods. Representative results. Similar results were obtained in two or more additional experiments with each ligand.

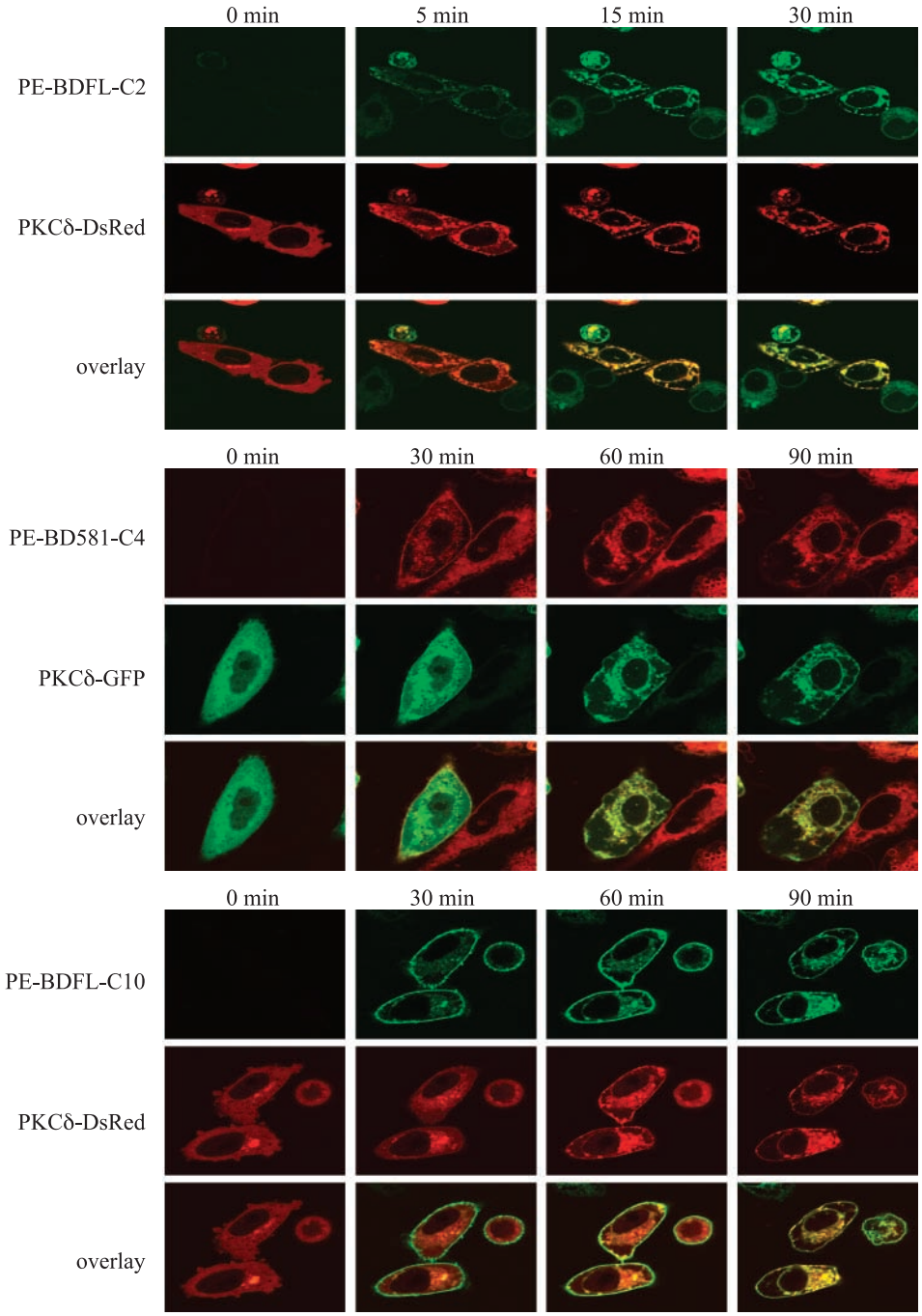

Figure 5. Real-time visualization of fluorescent phorbol ester with green- or red-tagged PKCδ. CHO cells expressing GFP- or DsRed-tagged PKCδ were incubated in 1 μmol/L fluorescent phorbol ester. Images were recorded by laser scanning confocal microscopy as described in Materials and Methods. Representative results are shown. Similar results were obtained in two or more additional experiments.

more slowly (37). Similarly, Szallasi et al. had shown that the lipophilic phorbol ester PMA was released from cells slowly, whereas the relatively hydrophilic phorbol esters PDBu and 12-deoxyphorbol 13-phenylacetate were released quickly (38), indicating that lipophilic phorbol esters persist longer in the cell.

The times measured for uptake of the fluorescent phorbol esters used in this study are modestly to considerably longer compared with the early report that 12-*O*-(12-dansylamino-dodecanoyl)-phorbol-13-acetate equilibrated in cells within 3 minutes (39). Our series of homologous fluorescent ligands show that the lipophilicity of a ligand has a marked influence on its rate of uptake. However, other parameters may influence the rate of uptake of a ligand, such as bulkiness of the molecule, degree of ionization, and/or localization of ionized functional groups.

Our experiments showed that the kinetics of uptake was dependent on serum, and more specifically, orosomucoid. A clear implication is that the presence of serum will influence the kinetics of biological response to the phorbol

ester. The effect on uptake was not unexpected because early studies had shown that sera of various mammalian species directly bound biologically active phorbol esters and inhibited phorbol ester binding to cellular receptor (40–42). It is important that the effect of serum binding be considered in extrapolation from cellular results to therapeutic applications for the phorbol esters.

The fluorescent phorbol esters of different lipophilicities allowed us to visualize the equilibrium distribution of each drug inside of Chinese hamster ovary (CHO) cells by using laser scanning confocal microscopy. We observed partitioning of phorbol ester to intracellular membranes around the perinuclear area. This pattern closely resembles that previously described for 12-*O*-(12-dansylaminododecanoyl)-phorbol-13-acetate (39). Phorbol ester did not concentrate in the nucleus, and surprisingly, little or no phorbol ester was visualized in the plasma membrane. The patterns of intracellular distribution were the same regardless of the lipophilicity of the phorbol ester, although the rate of uptake was significantly slower for lipophilic phorbol esters. These results strongly argue that different distributions of phorbol esters do not account for the different patterns of PKCδ localization that we had described previously (26).

Experiments with fluorescent phorbol ester and green or red tagged RasGRP3, PKCα, and PKCδ allowed us to visualize the colocalization and comigration of receptor and ligand. RasGRP3 and phorbol ester colocalized to a high degree in the perinuclear region, and this colocalization or pattern of distribution was the same regardless of the lipophilicity of the ligand, although the lipophilic phorbol esters both penetrated and induced translocation much more slowly. Phorbol ester induced patchy translocation of PKCα to the cytoplasm and initially colocalized with PKCα but then, as ligand entered the cell, the predominant location of the ligand shifted to the perinuclear area at a rate which was slower for the lipophilic phorbol esters.

An important conclusion is thus that the selectivity of PKCα for the plasma membrane is not driven by selective localization of phorbol ester to that location. Rather, although phorbol ester stimulates the translocation, the plasma membrane selectivity of PKCα is dominated by other factors. Presumably, the same conclusion holds true for other PKC isoforms, which also selectively translocate to the plasma membrane, such as PKCγ (27).

The pattern of localization of PKCδ was shown to be dependent on the lipophilicity of the phorbol ester. The hydrophilic phorbol esters colocalized with PKCδ at the perinuclear region, whereas the hydrophobic phorbol esters initially colocalized with PKCδ at the cytoplasm, progressing to perinuclear colocalization over time. The visible proportion of cytoplasmic to perinuclear colocalization also seemed to be a consistent function of lipophilicity of the phorbol ester.

Because phorbol esters of different lipophilicities exhibit the same pattern of localization within nontransfected CHO cells, equilibrium localization of phorbol ester is unlikely to be a determining factor of the pattern of PKCδ translocation. More likely, it is the lipophilicity-dependent variation in rate of uptake and persistence of phorbol ester within lipid membranes that mediates the different translocation patterns that are seen with PKCδ. Because of its slow penetration and slow rate of release from the receptor after binding, the lipophilic phorbol esters would first be present at the plasma membrane and trapped there with receptor before accumulating internally.

One strategy for the development of ligands with differential selectivities within the PKC pathway has been to develop ligands that show different intrinsic recognition for PKC isoforms in *in vitro* binding assays. The present studies suggest a second approach. Compounds of different rates of penetration will give different proportions of activation of PKC isoforms at the plasma membrane and at internal membranes. Whereas a rapidly penetrating ligand will stimulate PKCα at the plasma membrane and PKCδ at internal membranes, a slowly penetrating ligand will initially stimulate both at the plasma membrane. Because the site of stimulation will determine which substrates are phosphorylated, different patterns of response would be predicted.

It is clear that ligands for PKC, which induce different patterns of biological response, can drive different rates and patterns of PKC translocation (25, 27). Likewise, molecular alterations in PKC, which affect its localization (43), or treatments with peptides that interfere with its association with binding partners (44) affect biological activity. It remains for future studies, however, to trace mechanistic links between localization kinetics and the modulation of the complex biological end points observed for structurally different phorbol derivatives.

The development of ligands for PKCs and RasGRPs is exciting due to the role of these receptors in cell proliferation and apoptosis, making them attractive targets for cancer chemotherapy. Because of the complexity of PKC and RasGRP signaling, which is isoform, cell type, and context dependent, the opportunity exists to develop drugs with specificity. This study showed that the lipophilicity of a phorbol ester is an important determinant in its uptake kinetics and persistence in cellular membranes. This, in turn, affected the translocation kinetics of the three DAG receptors that we tested and is predicted to impact downstream signaling events.

Acknowledgments

We thank Nancy E. Lewin and Larry V. Pearce for their excellent technical assistance with the PDBu competition assays, Stephen Wincovitch for sharing his expertise with confocal microscopy, and Patricia S. Lorenzo for the GFP-PKCα plasmid.

References

1. Newton AC. Protein kinase C: structure, function, and regulation. J Biol Chem 1995;270:28495–8.

2. Mochly-Rosen D, Kauvar LM. Pharmacological regulation of network kinetics by protein kinase C localization. Semin Immunol 2000;12:55–61.

3. Kazanietz MG. Eyes wide shut: protein kinase C isozymes are not the only receptors for the phorbol ester tumor promoters. Mol Carcinog 2000;28:5–11.

4. Teixeira C, Stang SL, Zheng Y, Beswick NS, Stone JC. Integration of DAG signaling systems mediated by PKC-dependent phosphorylation of RasGRP3. Blood 2003;102:1414 – 20.

5. Lorenzo PS, Beheshti M, Pettit GR, Stone JC, Blumberg PM. The guanine nucleotide exchange factor RasGRP is a high-affinity target for diacylglycerol and phorbol esters. Mol Pharmacol 2000; 57:840 – 6.

6. Lorenzo PS, Kung JW, Bottorff DA, Garfield SH, Stone JC, Blumberg PM. Phorbol esters modulate the Ras exchange factor RasGRP3. Cancer Res 2001;61:943 – 9.

7. Hurley JH, Newton AC, Parker PJ, Blumberg PM, Nishizuka Y. Taxonomy and function of C1 protein kinase C homology domains. Protein Sci 1997;6:477 – 80.

8. Newton AC. Protein kinase C. Seeing two domains. Curr Biol 1995;5:973 – 6.

9. Mackay HJ, Twelves CJ. Protein kinase C: a target for anticancer drugs? Endocr Relat Cancer 2003;10:389 – 96.

10. Brodie C, Blumberg PM. Regulation of cell apoptosis by protein kinase C δ. Apoptosis 2003;8:19 – 27.

11. Tonetti DA, Chisamore MJ, Grdina W, Schurz H, Jordan VC. Stable transfection of protein kinase C α cDNA in hormone-dependent breast cancer cell lines. Br J Cancer 2000;83:782 – 91.

12. Krasagakis K, Lindschau C, Fimmel S, et al. Proliferation of human melanoma cells is under tight control of protein kinase C α. J Cell Physiol 2004;199:381 – 7.

13. O'Brian CA, Ward NE, Stewart JR, Chu F. Prospects for targeting protein kinase C isozymes in the therapy of drug-resistant cancer—an evolving story. Cancer Metastasis Rev 2001;20:95 – 100.

14. Clamp A, Jayson GC. The clinical development of the bryostatins. Anticancer Drugs 2002;13:673 – 83.

15. Strair RK, Schaar D, Goodell L, et al. Administration of a phorbol ester to patients with hematological malignancies: preliminary results from a phase I clinical trial of 12-*O*-tetradecanoylphorbol-13-acetate. Clin Cancer Res 2002;8:2512 – 8.

16. Ogbourne SM, Suhrbier A, Jones B, et al. Antitumor activity of 3-ingenyl angelate: plasma membrane and mitochondrial disruption and necrotic cell death. Cancer Res 2004;64:2833 – 9.

17. Roychowdhury D, Lahn M. Antisense therapy directed to protein kinase C-α (Affinitak, LY900003/ISIS 3521): potential role in breast cancer. Semin Oncol 2003;30:30 – 3.

18. Hanauske AR, Sundell K, Lahn M. The role of protein kinase C-α (PKC-α) in cancer and its modulation by the novel PKC-α-specific inhibitor aprinocarsen. Curr Pharm Des 2004;10:1923 – 36.

19. Mandlekar S, Kong AN. Mechanisms of tamoxifen-induced apoptosis. Apoptosis 2001;6:469 – 77.

20. Roaten JB, Kazanietz MG, Caloca MJ, et al. Interaction of the novel anthracycline antitumor agent *N*-benzyladriamycin-14-valerate with the C1-regulatory domain of protein kinase C: structural requirements, isoform specificity, and correlation with drug cytotoxicity. Mol Cancer Ther 2002;1:483 – 92.

21. Ishii H, Koya D, King GL. Protein kinase C activation and its role in the development of vascular complications in diabetes mellitus. J Mol Med 1998;76:21 – 31.

22. Gustafson KR, Cardellina JH, McMahon JB, et al. A nonpromoting phorbol from the Samoan medicinal plant *Homalanthus nutans* inhibits cell killing by HIV-1. J Med Chem 1992;35:1978 – 86.

23. Bocklandt S, Blumberg PM, Hamer DH. Activation of latent HIV-1 expression by the potent anti-tumor promoter 12-deoxyphorbol 13-phenylacetate. Antiviral Res 2003;59:89 – 98.

24. Oancea E, Meyer T. Protein kinase C as a molecular machine for decoding calcium and diacylglycerol signals. Cell 1998;95:307 – 18.

25. Wang QJ, Bhattacharyya D, Garfield S, Nacro K, Marquez VE, Blumberg PM. Differential localization of protein kinase C δ by phorbol esters and related compounds using a fusion protein with green fluorescent protein. J Biol Chem 1999;274:37233 – 9.

26. Wang QJ, Fang TW, Fenick D, et al. The lipophilicity of phorbol esters as a critical factor in determining the pattern of translocation of protein kinase C δ fused to green fluorescent protein. J Biol Chem 2000;275:12136 – 46.

27. Shirai Y, Sakai N, Saito N. Subspecies-specific targeting mechanism of protein kinase C. Jpn J Pharmacol 1998;78:411 – 7.

28. Marquez VE, Blumberg PM. Synthetic diacylglycerols (DAG) and DAG-lactones as activators of protein kinase C (PK-C). Acc Chem Res 2003;36:434 – 43.

29. Sambrook J, Russell DW. Molecular cloning. 3rd ed. Cold Spring Harbor (NY): Cold Spring Harbor Laboratory; 2001. 3 vols.

30. Lewin NE, Blumberg PM. [^{3}H]Phorbol 12,13-dibutyrate binding assay for protein kinase C and related proteins. Methods Mol Biol 2003;233:129 – 56.

31. Kazanietz MG, Krausz KW, Blumberg PM. Differential irreversible insertion of protein kinase C into phospholipid vesicles by phorbol esters and related activators. J Biol Chem 1992;267:20878 – 86.

32. Meylan WM, Howard PH. Atom/fragment contribution method for estimating octanol-water partition coefficients. J Pharm Sci 1995;84: 83 – 92.

33. Slater SJ, Ho C, Stubbs CD. The use of fluorescent phorbol esters in studies of protein kinase C-membrane interactions. Chem Phys Lipids 2002;116:75 – 91.

34. Karolin J, Johannson LB-A, Strandberg L, Ny T. Fluorescence and absorption spectroscopic properties of dypyrrometheneboron difluoride (BODIPY) derivatives in liquids, lipid membranes, and proteins. J Am Chem Soc 1994;116:7801 – 6.

35. Jacobson K, Wenner CE, Kemp G, Papahadjopoulos D. Surface properties of phorbol esters and their interaction with lipid monolayers and bilayers. Cancer Res 1975;35:2991 – 5.

36. Sharkey NA, Blumberg PM. Highly lipophilic phorbol esters as inhibitors of specific [^{3}H]phorbol 12,13-dibutyrate binding. Cancer Res 1985;45:19 – 24.

37. Murphy TV, Prountzos C, Kotsonis P, Iannazzo L, Majewski H. Structural determinants of phorbol ester binding in synaptosomes: pharmacokinetics and pharmacodynamics. Eur J Pharmacol 1999;381: 77 – 84.

38. Szallasi Z, Smith CB, Blumberg PM. Dissociation of phorbol esters leads to immediate redistribution to the cytosol of protein kinases C α and C δ in mouse keratinocytes. J Biol Chem 1994;269:27159 – 62.

39. Tran PL, Deugnier MA. Intracellular localization of 12-*O*-3-*N*-dansylamino TPA in C3H/10T1/2 mouse cell line. Carcinogenesis 1985;6:433 – 9.

40. Horowitz AD, Greenebaum E, Weinstein IB. Identification of receptors for phorbol ester tumor promoters in intact mammalian cells and of an inhibitor of receptor binding in biologic fluids. Proc Natl Acad Sci U S A 1981;78:2315 – 9.

41. Horowitz AD, Greenebaum E, Nicolaides M, Woodward K, Weinstein IB. Inhibition of phorbol ester-receptor binding by a factor from human serum. Mol Cell Biol 1982;2:545 – 53.

42. Shoyab M, Todaro GJ. Partial purification and characterization of a binding protein for biologically active phorbol and ingenol esters from murine sera. J Biol Chem 1982;257:439 – 45.

43. Walker SD, Murray NR, Burns DJ, Fields AP. Protein kinase C chimeras: catalytic domains of α and β II protein kinase C contain determinants for isotype-specific function. Proc Natl Acad Sci U S A 1995;92:9156 – 60.

44. Schechtman D, Mochly-Rosen D. Adaptor proteins in protein kinase C-mediated signal transduction. Oncogene 2001;20:6339 – 47.

Molecular Cancer Therapeutics

Role of phorbol ester localization in determining protein kinase C or RasGRP3 translocation: Real-time analysis using fluorescent ligands and proteins

Derek C. Braun, Yeyu Cao, Shaomeng Wang, et al.

Mol Cancer Ther 2005;4:141-150.